Accepted Manuscript

Activation of TRPV3 inhibits lipogenesis and stimulates production of inflammatory mediators in human sebocytes – a putative contributor to dry skin dermatoses

Magdolna Szántó, Attila Oláh, Attila Gábor Szöllősi, Kinga Fanni Tóth, Edit Páyer, Nóra Czakó, Ágnes Pór, Ilona Kovács, Christos C. Zouboulis, Lajos Kemény, Tamás Bíró, Balázs István Tóth

PII: S0022-202X(18)32460-6

DOI: 10.1016/j.jid.2018.07.015

Reference: JID 1532

To appear in: *The Journal of Investigative Dermatology*

Received Date: 3 May 2017

Revised Date: 13 July 2018

Accepted Date: 13 July 2018

Please cite this article as: Szántó M, Oláh A, Szöllősi AG, Tóth KF, Páyer E, Czakó N, Pór Á, Kovács I, Zouboulis CC, Kemény L, Bíró T, Tóth BI, Activation of TRPV3 inhibits lipogenesis and stimulates production of inflammatory mediators in human sebocytes – a putative contributor to dry skin dermatoses, *The Journal of Investigative Dermatology* (2018), doi: 10.1016/j.jid.2018.07.015.

TITLE PAGE

Activation of TRPV3 inhibits lipogenesis and stimulates production of inflammatory mediators in human sebocytes – a putative contributor to dry skin dermatoses

by

Magdolna Szántó[1*], Attila Oláh[1*], Attila Gábor Szöllősi[1], Kinga Fanni Tóth[1], Edit Páyer[1,2], Nóra Czakó[1], Ágnes Pór[3], Ilona Kovács[3], Christos C. Zouboulis[4], Lajos Kemény[5], Tamás Bíró[1,6,**], Balázs István Tóth[1,#,**]

[1]Department of Physiology, Faculty of Medicine, University of Debrecen, Debrecen, Hungary
[2]Department of Hematology, Faculty of Medicine, University of Debrecen, Debrecen, Hungary
[3]Department of Pathology, Gyula Kenézy Hospital, Debrecen, Debrecen, Hungary
[4]Deparments of Dermatology, Venereology, Allergology and Immunology, Dessau Medical Center, Theodore Fontane Medical University of Brandenburg, Dessau, Germany
[5]Department of Dermatology and Allergology, Faculty of Medicine, University of Szeged, Szeged, Hungary
[6]Department of Immunology, Faculty of Medicine, University of Debrecen, Debrecen, Hungary

*MSz and AO share first authorship

**TB an BIT contributed equally to the work as senior authors

[#]To whom correspondence should be addressed:

Balázs István Tóth, PhD
Department of Physiology, Faculty of Medicine
University of Debrecen
H-4032 Debrecen, Egyetem tér 1.
Office Phone: +36 52 411-717/54212
FAX: +36 52 255-116
Email: toth.istvan@med.unideb.hu

Transient receptor potential vanilloid 3 (TRPV3) was cloned from keratinocytes and described as a thermosensitive member of the transient receptor potential (TRP) ion channel family. Although its role in thermosensation is currently under debate, it is highly expressed in the epidermis and functions as a nonselective, Ca^{2+}-permeable cation channel (Huang et al. 2011; Nilius and Bíró 2013; Peier et al. 2002). Despite its high abundance in the skin, its genetic deletion only causes moderate, often strain- or gender-dependent cutaneous phenotypic modifications, such as formation of curly whiskers and wavy hair, defect in epidermal barrier functions and alterations in epidermal nitrate homeostasis (Cheng et al. 2010; Miyamoto et al. 2011). In contrast, gain-of-function mutations of TRPV3 result in dramatic cutaneous alterations associated with severely dry skin, dermatitis and hairless phenotype in both mice and rats (Asakawa et al. 2006; Xiao et al. 2008). Moreover, similar gain-of-function mutations of TRPV3 were found to play an etiological role in a rare human genodermatosis, Olmsted syndrome, characterized by periorofacial hyperkeratosis, hypotrichosis, alopecia and severe pruritus (He et al. 2015; Lin et al. 2012; Ni et al. 2016). Encouraged by these findings, we verified the role of TRPV3 in human hair growth control by inducing catagen in mechanistic studies (Borbíró et al. 2011) and, most recently, we also described the pro-inflammatory action of TRPV3 activation in human epidermal keratinocytes (Szöllősi et al. 2018), whereas others reported its role in dry skin-associated itching (Yoshioka et al. 2009). However, the extended inflammatory symptoms and the disrupted lipid barrier found both in rodents and human suggested that TRPV3-expressing skin cells other than keratinocytes might also be involved in the development of inflammatory skin conditions induced by TRPV3 hyperfunction. Therefore, in the current study, we investigated the expression and activation of TRPV3 in human sebocytes, which are important regulators of cutaneous homeostasis (Tóth et al. 2011).

Immunohistochemical analysis revealed that, like epidermal keratinocytes, human sebaceous glands (SG) express TRPV3 *in situ* (Figure 1a). Peripheral undifferentiated cells show stronger immunopositivity than centrally located terminally differentiated cells. We also demonstrated the presence of TRPV3 protein and mRNA transcripts in human SG-derived SZ95 sebocytes (Zouboulis et al. 1999), a widely accepted model cell line to study SG biology *in vitro* (Figure 1b-d). We observed that TRPV3 expression is decreased in post-confluent, more differentiated cultures compared to the highly proliferating preconfluent cultures (Figure 1c-d). Importantly, the synthetic TRPV3 activator 2-aminoethoxydiphenyl-borate (2-APB), as well as the plant-derived carvacrol evoked marked elevation of the intracellular Ca^{2+} concentration (Figure 1e) suggesting that TRPV3 is, indeed, functionally expressed in human sebocytes. The evoked Ca^{2+} signals were practically abolished in the presence of the general TRP channel blocker ruthenium red, but were not affected by either AMG9810 or HC067047, selective antagonists of the closely related channels TRPV1 and TRPV4, respectively (Figure 1f), which channels are also functionally expressed by sebocytes (Oláh et al. 2014; Tóth et al. 2009). Since highly specific TRPV3 activators and inhibitors are not available commercially, we then investigated the effect of RNAi-based silencing of TRPV3 expression on Ca^{2+} signals. Transfection of the sebocytes with siRNA targeting TRPV3 resulted in a partial, yet marked decrease of the channel expression (Figure S1) compared to the scrambled RNA-transfected cells, and significantly suppressed the amplitude and the rate of rise of the agonists evoked Ca^{2+} signals (Figure 1g-h); these data provided strong evidence for the activation of TRPV3 by the applied compounds. Higher concentrations of the activators reduced the living cell number in 24 hours, but lower concentrations (still able to evoke Ca^{2+} signals) did not influence the viability of

sebocytes (Figure S2), confirming previous results on Ca^{2+} signaling-induced sebocyte apoptosis (Zouboulis et al. 2017).

Since sebaceous lipids essentially contribute to the epidermal barrier functions, we also investigated the influence of TRPV3 on lipid synthesis in SZ95 cells. Activation of TRPV3 with non-cytotoxic concentrations of 2-APB and carvacrol decreased lipid synthesis during arachidonic acid (AA)-induced differentiation of scrambled RNA-transfected cells used as control. Importantly, TRPV3 agonists were less effective to suppress AA induced lipid synthesis in cells transfected with siRNA targeting TRPV3 (Figure 2a). Moreover, AA was slightly, but significantly more effective in TRPV3-silenced cells suggesting that basal activity of TRPV3 also negatively regulates AA-induced lipid synthesis. Notably, the effect of TRPV3 agonists was not restricted to AA-induced lipid synthesis: they also inhibited the lipogenic effect of the endocannabinoid anandamide, and of the combination of linoleic acid and testosterone, as well as they slightly decreased basal lipid synthesis of non-transfected sebocytes (Figure S3). Moreover, carvacrol did not induce cellular differentiation as it affected cellular granulation neither under control conditions nor in AA-treated cells. However, carvacrol selectively inhibited the AA induced accumulation of cellular lipids which effect was prevented by ruthenium red indicating that indeed TRPV3 mediates the effect (Figure S4a). Simultaneously, carvacrol downregulated peroxisome proliferator-activated receptor γ (PPARγ) and nuclear receptor interacting protein 1 (NRIP1), important positive regulators of sebaceous lipid synthesis (Dozsa et al. 2014; Oláh et al. 2014). These results suggested that TRPV3 mediated Ca^{2+} signaling generally inhibits lipid synthesis of sebocytes, independently of the activated lipogenic pathways, confirming a current study of our group on the role of Ca^{2+} signaling in human sebocytes using another experimental setting (Zouboulis et al. 2017). Our data are consistent

with our previous findings as TRPV1 and TRPV4 activation by capsaicin and cannabidiol, respectively, inhibited sebaceous lipid synthesis (Oláh et al. 2014; Tóth et al. 2009).

Beyond lipid synthesis, SGs play an important role in the regulation of cutaneous immune functions (Tóth et al. 2011). Therefore, we also assessed the effect of TRPV3 activation on cytokine expression of SZ95 sebocytes. Our findings revealed that transcription of several pro-inflammatory cytokines was unambiguously triggered by the TRPV3 agonist carvacrol within 6 hours (Figure 2b) although during this time, 2-APB was ineffective. To assess the TRPV3 specificity of the carvacrol treatment, we repeated the experiments on TRPV3-silenced SZ95 sebocytes. In this condition, we found a reduced effect of the activator compared to scrambled RNA-transfected cells (Figure 2c), again arguing for the involvement of TRPV3 in mediating the effect of carvacrol. Moreover, we found that not only the expression, but the release of some pro-inflammatory cytokines was also decreased by specific TRPV3 RNAi in carvacrol-treated sebocytes (Figure 2c).

Taken together, our findings suggest that sebocytes might be involved in the pathogenesis of dry skin-associated inflammatory dermatoses linked to TRPV3 hyperactivity. Furthermore, our pre-clinical findings introduce TRPV3 as a previously unreported negative regulator of sebaceous lipid synthesis with a marked pro-inflammatory effect. Further clinical studies are urged to assess the clinical efficacy of TRPV3 inhibitors on the therapeutic management of certain inflammatory skin conditions.

CONFLICT OF INTEREST

CCZ owns an international patent on the SZ95 sebaceous gland cell line (WO2000046353). The other authors state no conflict of interest.

ACKNOWLEDGEMENTS

The presented work was supported through the New National Excellence Program of the Ministry of Human Capacities, by a grant from the University of Debrecen to MS and by other Hungarian research grants (NKFI K_105369, K_120187, PD_121138, PD_121360, FK_125055, GINOP-2.3.2-15-2016-00050). MS, OA and BIT are recipients of the János Bolyai research scholarship of the Hungarian Academy of Sciences.

REFERENCES-

Asakawa M, Yoshioka T, Matsutani T, Hikita I, Suzuki M, Oshima I, et al. Association of a mutation in TRPV3 with defective hair growth in rodents. J. Invest. Dermatol. 2006;126(12):2664–72

Borbíró I, Lisztes E, Tóth BI, Czifra G, Oláh A, Szöllosi AG, et al. Activation of transient receptor potential vanilloid-3 inhibits human hair growth. J. Invest. Dermatol. 2011;131(8):1605–14

Cheng X, Jin J, Hu L, Shen D, Dong X-P, Samie MA, et al. TRP channel regulates EGFR signaling in hair morphogenesis and skin barrier formation. Cell. 2010;141(2):331–43

Dozsa A, Dezso B, Toth BI, Bacsi A, Poliska S, Camera E, et al. PPARγ-mediated and arachidonic acid-dependent signaling is involved in differentiation and lipid production of human sebocytes. J. Invest. Dermatol. 2014;134(4):910–20

He Y, Zeng K, Zhang X, Chen Q, Wu J, Li H, et al. A gain-of-function mutation in TRPV3 causes focal palmoplantar keratoderma in a Chinese family. J. Invest. Dermatol. 2015;135(3):907–9

Huang SM, Li X, Yu Y, Wang J, Caterina MJ. TRPV3 and TRPV4 ion channels are not major contributors to mouse heat sensation. Mol. Pain. 2011;7:37

Lin Z, Chen Q, Lee M, Cao X, Zhang J, Ma D, et al. Exome sequencing reveals mutations in TRPV3 as a cause of Olmsted syndrome. Am. J. Hum. Genet. 2012;90(3):558–64

Miyamoto T, Petrus MJ, Dubin AE, Patapoutian A. TRPV3 regulates nitric oxide synthase-independent nitric oxide synthesis in the skin. Nat. Commun. 2011;2:369

Ni C, Yan M, Zhang J, Cheng R, Liang J, Deng D, et al. A novel mutation in TRPV3 gene causes atypical familial Olmsted syndrome. Sci. Rep. 2016;6:21815

Nilius B, Bíró T. TRPV3: a "more than skinny" channel. Exp. Dermatol. 2013;22(7):447–52

Oláh A, Tóth BI, Borbíró I, Sugawara K, Szöllõsi AG, Czifra G, et al. Cannabidiol exerts sebostatic and antiinflammatory effects on human sebocytes. J. Clin. Invest. 2014;124(9):3713–24

Peier AM, Reeve AJ, Andersson DA, Moqrich A, Earley TJ, Hergarden AC, et al. A heat-sensitive TRP channel expressed in keratinocytes. Science. 2002;296(5575):2046–9

Szöllősi AG, Vasas N, Angyal Á, Kistamás K, Nánási PP, Mihály J, et al. Activation of TRPV3 Regulates Inflammatory Actions of Human Epidermal Keratinocytes. J. Invest. Dermatol. 2018;138(2):365–74

Tóth BI, Géczy T, Griger Z, Dózsa A, Seltmann H, Kovács L, et al. Transient receptor potential vanilloid-1 signaling as a regulator of human sebocyte biology. J. Invest. Dermatol. 2009;129(2):329–39

Tóth BI, Oláh A, Szöllosi AG, Czifra G, Bíró T. “Sebocytes’’ makeup": novel mechanisms and concepts in the physiology of the human sebaceous glands.” Pflugers Arch. 2011;461(6):593–606

Xiao R, Tian J, Tang J, Zhu MX. The TRPV3 mutation associated with the hairless phenotype in rodents is constitutively active. Cell Calcium. 2008;43(4):334–43

Yoshioka T, Imura K, Asakawa M, Suzuki M, Oshima I, Hirasawa T, et al. Impact of the Gly573Ser substitution in TRPV3 on the development of allergic and pruritic dermatitis in mice. J. Invest. Dermatol. 2009;129(3):714–22

Figure legends:

Figure 1. Human sebocytes express functional TRPV3 ion channels

a, Immunohistochemical staining of TRPV3 (3,3'-diaminobenzidine (DAB), brown precipitation) on human sebaceous glands (SG) and epidermis. NC, negative control. White and yellow arrowheads indicate undifferentiated and terminally differentiated cells, respectively. Scale bar = 50 µm in each image. b, Immunocytochemical staining of TRPV3 (fluorescein isothiocyanate (FITC), green fluorescence) on SZ95 sebocytes. Blue: nuclei (4',6-diamidino-2-phenylindole (DAPI)). Scale bar = 25 µm. c, Western blot analysis of protein lysates of human epidermal keratinocytes (KC) and SZ95 sebocytes from pre- and postconfluent (pre and post, respectively) cultures followed by immunolabeling with anti-TRPV3 antibody. MW, molecular weight in kDa as indicated. Expected molecular weight of recombinant TRPV3 is ca. 91 kDa (http://www.uniprot.org/uniprot/Q2M3L1). Multiple bands may refer to uncharacterized post-translational modifications, e.g. glycosylation, and multimerization of channel subunits. d, Relative expression of TRPV3 transcripts in pre- and postconfluent SZ95 sebocyte cultures. e, Representative Ca^{2+} signals on SZ95 sebocytes evoked by TRPV3 agonists 2-APB and carvacrol in the presence or absence of ruthenium red (RR) applied as indicated. f, Statistical analysis of the amplitudes of the Ca^{2+} signals in various conditions as indicated. N=6 in each group. ***$p<0.001$ compared to the control and $^{###}p<0.001$ between the indicated groups as determined by ANOVA and Bonferroni *post hoc* test. g, Representative Ca^{2+} signals evoked by TRPV3 agonists 2-APB (200 µM) and carvacrol (500 µM) on human SZ95 sebocytes transfected with scrambled RNA (scrRNA) or siRNA targeting TRPV3 (siRNA-TRPV3). h, Statistical analysis on the amplitude and the rate of rise of the 2-APB and carvacrol induced Ca^{2+} signals in sebocytes transfected with scrambled or siRNA targeting TRPV3, as indicated. N=5 in each

group. $^{+}p<0.05$ and $^{++}p<0.01$ between the indicated groups as determined by two-tailed Student's t-test for independent samples.

Figure 2. Activation of TRPV3 inhibits lipid synthesis associated with sebaceous differentiation and induces the synthesis and release of pro-inflammatory cytokines

a. Quantitative Nile Red staining of neutral lipids in scrambled RNA (scr RNA) and TRPV3 targeting siRNA (siRNA-TRPV3) transfected SZ95 sebocytes treated with arachidonic acid and TRPV3 agonists for 24 hours, as indicated. N≥4 in each group. ***p<0.001 between the indicated groups as determined by One-way ANOVA and Bonferroni *post hoc* test. b. Relative expression of pro-inflammatory cytokine transcripts in SZ95 sebocytes after a 6-hour-long treatment with vehicle (used as control) or TRPV3 agonists, as indicated. $^{\#}p<0.05$ and $^{\#\#\#}p<0.001$ compared to the vehicle treated control using One-way ANOVA and Dunnett *post hoc* test. PPIA, Peptidylprolyl Isomerase A or cyclophyllin A used as endogenous control reference gene. c. Carvacrol (Carv, 500 µM, 6 hrs) induced changes in relative expression of pro-inflammatory cytokine genes (determined by Q-PCR). in scrambled RNA (scr RNA) and TRPV3 specific siRNA (siRNA-TRPV3) transfected SZ95 sebocytes. d. Release of pro-inflammatory cytokines (determined from supernatants using ELISA) following the same treatments as indicated in panel c. $^{+}p<0.05$, $^{++}p<0.01$ and $^{+++}p<0.001$ between scrambled RNA and TRPV3 specific siRNA transfected and $^{\#}p<0.05$ between vehicle and carvacrol treated cells as determined by two-tailed Student's t-test for independent samples. n.s., non-significant.

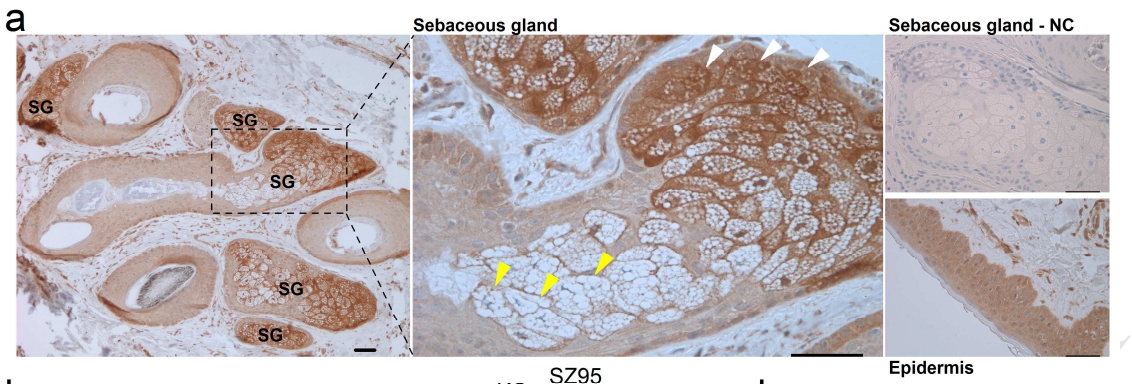
a
Sebaceous gland
Sebaceous gland - NC
SG
SG
SG
SG
SG
Epidermis

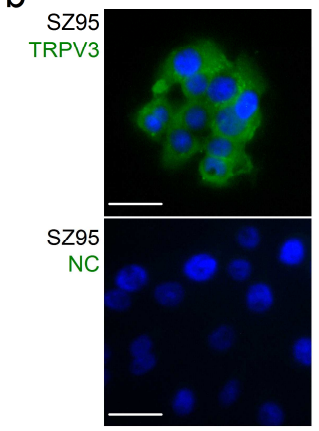
b
SZ95
TRPV3
SZ95
NC

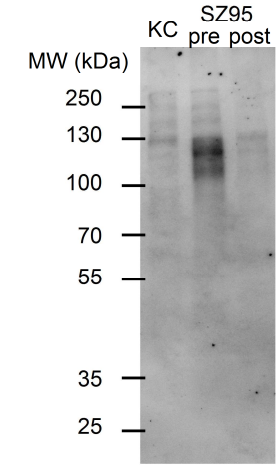
c
KC
SZ95
pre post
MW (kDa)
250
130
100
70
55
35
25

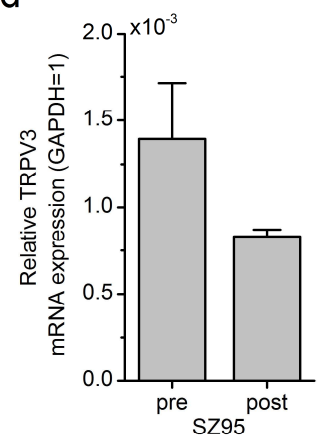
d
x10-3
2.0
1.5
1.0
0.5
0.0
Relative TRPV3
mRNA expression (GAPDH=1)
pre
post
SZ95

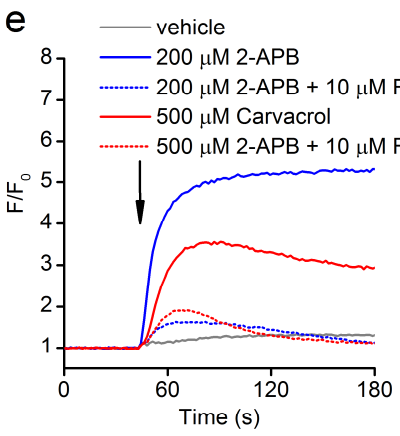
e
vehicle
200 μM 2-APB
200 μM 2-APB + 10 μM RR
500 μM Carvacrol
500 μM 2-APB + 10 μM RR
F/F0
Time (s)

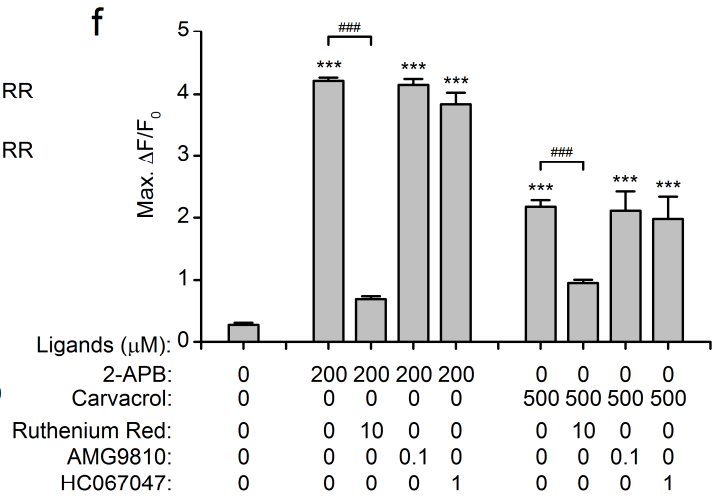
f
Max. ΔF/F0
###
***
Ligands (μM):
2-APB:
Carvacrol:
Ruthenium Red:
AMG9810:
HC067047:

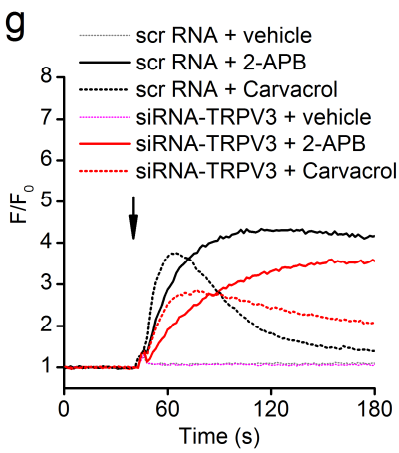
g
scr RNA + vehicle
scr RNA + 2-APB
scr RNA + Carvacrol
siRNA-TRPV3 + vehicle
siRNA-TRPV3 + 2-APB
siRNA-TRPV3 + Carvacrol
F/F0
Time (s)

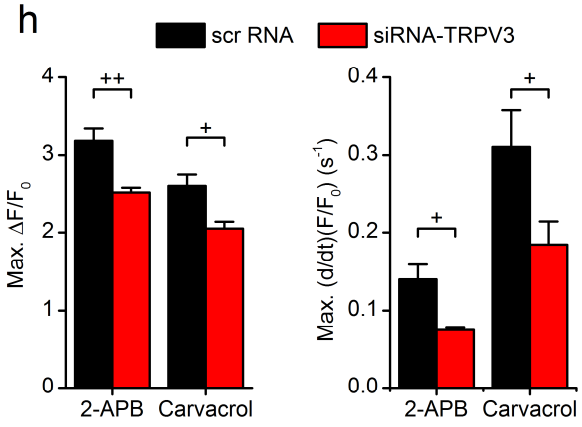
h
scr RNA
siRNA-TRPV3
Max. ΔF/F0
Max. (d/dt)(F/F0) (s-1)
2-APB
Carvacrol

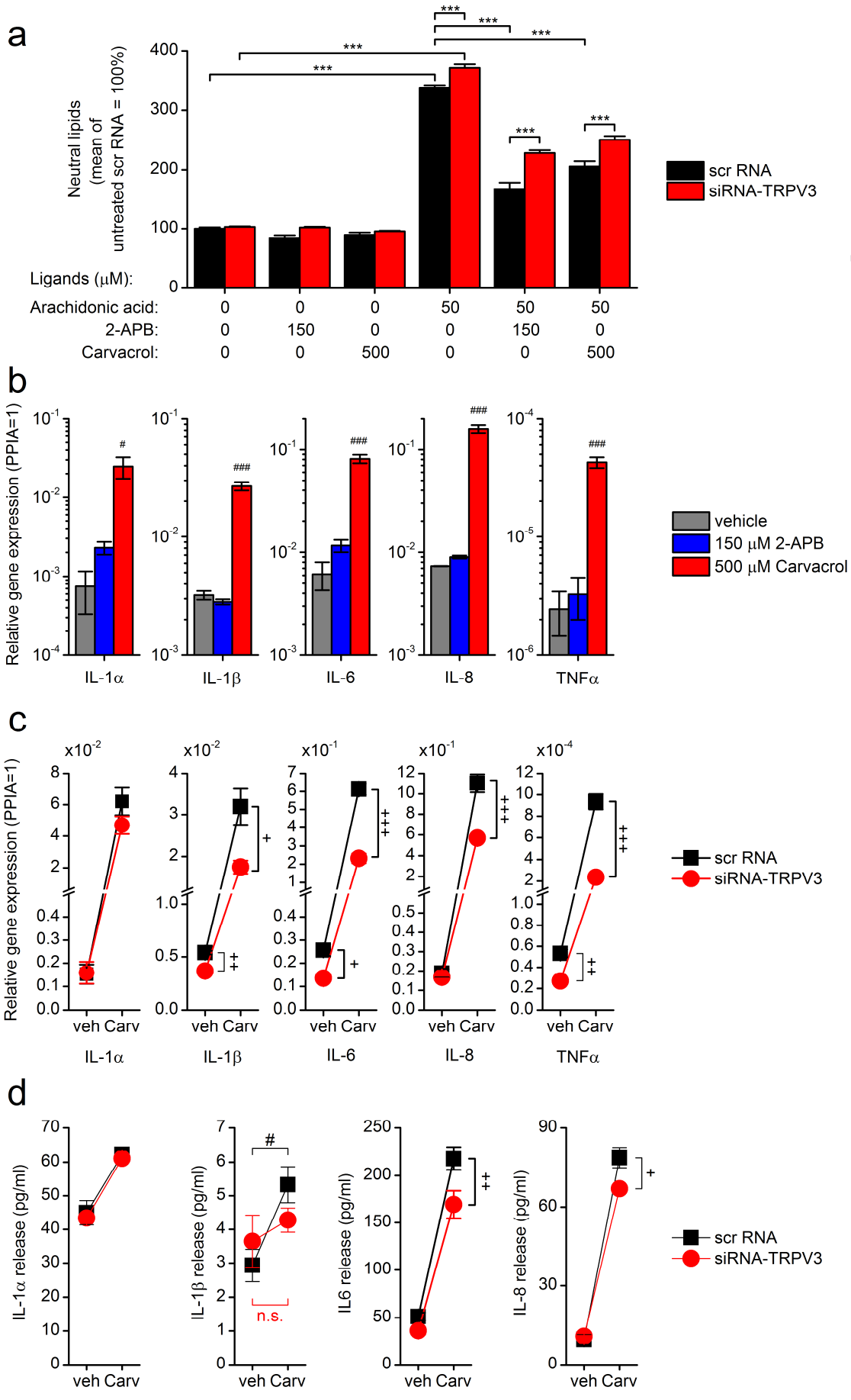
a
Neutral lipids (mean of untreated scr RNA = 100%)
400
300
200
100
0
***
Ligands (μM):
Arachidonic acid: 0 0 0 50 50 50
2-APB: 0 150 0 0 150 0
Carvacrol: 0 0 500 0 0 500
scr RNA
siRNA-TRPV3
b
Relative gene expression (PPIA=1)
#
###
IL-1α
IL-1β
IL-6
IL-8
TNFα
vehicle
150 μM 2-APB
500 μM Carvacrol
c
Relative gene expression (PPIA=1)
x10-2
x10-1
x10-4
veh Carv
IL-1α
IL-1β
IL-6
IL-8
TNFα
scr RNA
siRNA-TRPV3
d
IL-1α release (pg/ml)
IL-1β release (pg/ml)
IL6 release (pg/ml)
IL-8 release (pg/ml)
n.s.
veh Carv
scr RNA
siRNA-TRPV3

SUPPLEMENTARY MATERIAL

Supplementary materials and methods

Materials

Carvacrol, 2-Aminoethoxydiphenyl borate (2-APB), arachidonic acid (AA), testosterone, linoleic acid, and N-arachidonoylethanolamine (anandamide, AEA) were obtained from Sigma-Aldrich whereas AMG 9810 and HC067047 were from Tocris Bioscience (Bristol, UK). Ruthenium red was purcheased from Research Biochemicals International (Natick, MA, USA).

Cell culturing

Human immortalized SZ95 sebocytes, originated from human facial sebaceous glands (Zouboulis et al. 1999), were cultured in Sebomed® Basal Medium (Merck-Millipore, Berlin, Germany) supplemented with 10% fetal bovine serum (Life Technologies Corporation, Carlsbad, CA, USA), 1 mM $CaCl_2$, 5 ng/ml human recombinant epidermal growth factor (Sigma-Aldrich), 50 IU/ml penicillin and 50 μg/ml streptomycin (both from PPA Laboratories, Pasching, Austria). The medium was changed every other day, and cells were sub-cultured at 60-70% confluence. Human keratinocytes were isolated from skin samples of healthy individuals undergoing dermatosurgery following written informed consent adhering to Helsinki guidelines, and after obtaining Institutional Research Ethics Committee's and Government Office for Hajdú-Bihar County's permission (protocol No.: DE OEC RKEB/IKEB 3721-2012). Primary keratinocytes were handled and cultured as described previously (Szöllősi et al. 2018).

Immunocytochemistry

SZ95 sebocytes, seeded and cultured on sterile coverslips in 24-well plates, were fixed in ice-cold acetone (VWR, Radnor, PA, USA) for 5 min and then permeabilized by 0.1% Triton-X-100 in phosphate-buffered saline (PBS; 115 mM NaCl, 20 mM Na_2PO_4, pH 7.4; all from Sigma-Aldrich) for 10 min. After washing in PBS and blocking in 1% bovine serum albumin (BSA, Sigma-Aldrich) in PBS for 30 min, cells were incubated with the TRPV3 (AbCam, Cambridge, UK) specific primary antibodies (produced in rabbit; dilution 1:200 in blocking solution; overnight incubation at 4°C). For fluorescence staining, slides were then incubated with fluorescein isothiocyanate (FITC)-conjugated goat IgG-specific secondary antibody (Life Technologies) for 60 min (dilution 1:200), and the nuclei of cells were visualized using 4',6-diamidino-2-phenylindole (DAPI, Vector Laboratories, Burlingame, CA, USA). Cells were examined on a Nikon Eclipse E600 fluorescent microscope (Nikon, Tokyo, Japan). As negative control, the primary antibody was omitted from the procedure.

Immunohistochemistry

The immunohistochemical investigation of TRPV3 was performed on formalin fixed paraffin embedded, skin samples rich in sebaceous glands, all diagnosed as trichilemmal cyst in Kenézy County Hospital (Debrecen, Hungary). Serial 4 μm thick sections were cut from paraffin blocks. Heat-induced antigen retrieval was performed on formalin fixed samples. EDTA buffer (Reanal, Hungary, 1 mM, pH 8.0) was applied in microwave oven for 15 min to unmask epitope of TRPV3. Endogenous peroxidase activity was blocked with 3% H_2O_2 (Sigma-Aldrich) for 10 minutes. After blocking, tissue sections were incubated with a specific rabbit primary antibody against TRPV3 (Alomone, Jerusalem, Israel, 1:500, 60 min). TRPV3 expression was detected with HRP labelled Polymer Anti Rabbit EnVision+ system (Dako, Glostrup, Denmark) following the manufacturers protocol TRPV3 staining was visualized with 3,3'-Diaminobenzidine (DAB, DAKO, Golstrup, Denmark), nuclei were counterstained with hematoxylin (Sigma-Aldrich) and tissue sections were finally mounted in permanent mounting medium (Histolab, Göteborg, Sweden). Negative controls were obtained by omitting the primary antibody.

Determination of intracellular lipids

For quantitative measurement of lipid content, cells (20,000 cells/well) were cultured in 96-well black-well/clear-bottom plates (Greiner Bio-One, Frickenhausen, Germany) in quadruplicates and were treated with compounds for 24 hours. Subsequently, supernatants were discarded and 100 μl of a 1 μg/ml Nile Red (Sigma-Aldrich) solution in PBS was added to every well. Fluorescence was measured on a FlexStation 3 multi-mode microplate reader (Molecular Devices, San Francisco, CA). Results are expressed as percentages of the relative fluorescence units in comparison with the controls using 485 nm excitation and 565 nm emission wavelengths for neutral lipids (Alestas et al. 2006; Dobrosi et al. 2008).

Determination of viability

Viability was determined by measuring the conversion of the 3-(4,5-dimethylthiazol-2-yl)-2,5-diphenyltetrazolium bromide (MTT, Sigma-Aldrich) to formazan by mitochondrial dehydrogenases. Cells were plated in 96-well plates (in 20,000 cells/well density) in quadruplicates and were treated with compounds for 24-hours. Cells were then incubated with 0.5 mg/ml MTT for 3 hours, subsequently colorimetric analysis of the concentration of formazan crystals took place according to the manufacturer's instruction.

Fluorescent Ca^{2+}-measurement

SZ95 sebocytes were seeded in 96-well black-well/clear-bottom plates (Greiner Bio-One) at a density of 20,000 cells/well. Cells were washed once with 1% BSA and 2.5 mM probenecid (both from Sigma-Aldrich) containing Hank's solution (136.8 mM NaCl, 5.4 mM KCl, 0.34 mM Na_2HPO_4, 0.44 mM KH_2PO_4, 0.81 mM $MgSO_4$, 1.26 mM $CaCl_2$, 5.56 mM glucose, 4.17 mM

$NaHCO_3$, pH 7.2, all from Sigma-Aldrich), and loaded with 1 μM Fluo-4 AM (Life Technologies) dissolved in Hank's solution (100 μl/well) at 37°C for 30 min, and were then washed three times with Hank's solution (100 μl/well). The plates were then placed in a FlexStation 3 multi-mode microplate reader (Molecular Devices), and changes in cytoplasmic Ca^{2+} concentration (reflected by changes in fluorescence at 490 nm excitation and 520 nm emission wavelengths) induced by various TRPV3 agonist in various conditions were monitored. Experiments were performed in multiple wells and data were obtained as F/F_0, where F_0 is the average fluorescence of the baseline (before compound application) and F is the actual fluorescence.

RNA isolation, reverse transcription, quantitative "real-time" PCR (Q-PCR)

Total RNA was isolated using TRIzol reagent (Life Technologies) according to the manufacturer's protocol, and the isolated RNA was quality-checked by Nanodrop-1000 Spectrophotometer (Thermo Scientific, Wilmington, DE, USA). 2 μg of total RNA were then reverse-transcribed into cDNA by using the High Capacity cDNA Reverse Transcription Kit (Life Technologies) according to the manufacturer's protocol. PCR amplification was performed by using the TaqMan primers and probes (assay ID-s: Hs00376854_m1 for TRPV3, Hs00985639_m1 for IL-6, Hs00174103_m1 for IL-8, Hs00174092_m1 for IL-1α, Hs00174128_m1 for TNFα, Hs00234592_m1 for PPARγ and Hs00942766_s1 for NRIP1) using the TaqMan universal PCR master mix protocol (Life Technologies). As internal controls, transcripts of peptidyl-prolyl isomerase A (Cylophylin A, PPIA) and Glyceraldehyde 3-phosphate dehydrogenase (GAPDH) were determined (assay ID-s: Hs99999904_m1 for PPIA and Hs99999905_m1 for GAPDH). The amount of the transcripts was normalized to those of the housekeeping gene using the ΔCT method.

Western blotting

Cells were harvested and homogenized in detergent mixture (50 mM TRIS HCl, 150 mM NaCl, 1% Triton X-100, 1% Igepal CA 630, 0.5% sodium deoxicholate), containing protease inhibitor cocktail (1:100, all from Sigma-Aldrich). After ultrasonic homogenization, the protein content of the resulting samples was determined with a BCA protein assay kit (Pierce, Rockford, IL, USA). Protein samples (30 μg/well) were subjected to SDS-PAGE (10% Mini Protean TGX gels, Bio-Rad, Hercules, CA, USA), and transferred to nitrocellulose membranes, by using Trans-Blot® Turbo™ Nitrocellulose Transfer Packs and Trans Blot Turbo System (both from Bio-Rad). Membranes were probed with the rabbit primary antibody against human TRPV3 (1: 200 dilution, Alomone Labs, Jerusalem, Israel), in PBS containing 1% dry milk and 0.1% Tween-20) overnight at 4°C. As a secondary antibody, horseradish peroxidase-conjugated anti-rabbit IgG antibody (1:1000, Sigma) was used and the immunoreactive bands were visualized by a SuperSignal West Pico or Femto Chemiluminescent Substrate-Enhanced Chemiluminescence kits (Pierce) using a Kodak Gel Logic 1500 Imaging System (Kodak, Tokyo, Japan). To assess equal loading, the membranes were re-probed by using rabbit-anti-tubulin antibody (1:1000, AbCam).

RNA interference

Cells were transfected at ≈70% confluence with specific Stealth RNAi oligonucleotides (40 nM, Invitrogen) against TRPV3 (ID: HSS175965), using Lipofectamine RNAiMax Transfection Reagent (Invitrogen). For controls, Stealth RNAi Negative Control Med GC Duplexes (scrambled RNA construct; Invitrogen) were employed. The efficacy of RNAi-driven ‘‘knock-down’’ was evaluated 48 hours after transfection by Western blotting and Q-PCR as described previously above.

Determination of cytokine release (ELISA)

Supernatants were collected from sebocytes exposed to various treatments. While RNA was isolated from the cells as described above, the supernatants were analyzed for human IL-1α, IL-1β, IL-6, IL-8/CXCL-8 and TNFα using commercially available ELISA kits (BD Biosciences, Franklin Lakes, NJ, USA) according to the manufacturer’s protocols. In brief, plates were coated with capture antibody diluted in coating buffer (0.1 M Na_2CO_3, pH 9.5 with 10 N NaOH) and incubated overnight at 4°C. Then plates were incubated with assay diluent (10% fetal bovine serum in PBS) at room temperature (RT) for 1 hour, while standard and sample dilutions were prepared in assay diluent. Concentration standards and samples were added into appropriate wells and incubated for 2 hrs at RT. After 2 hours, working detector (detection antibody + SAv-HRP reagent) was added to each well, and incubated for 1 hour at RT. After every step, plates were washed with wash buffer (0.05% Tween-20 in PBS). After washing, substrate solution (tetramethylbenzidine and hydrogen peroxide in citrate-buffer, pH 5.0) was added to every well for 30 minutes in the dark, followed by stop solution (2 N H_2SO_4). Absorbance was read at 405 nm within 30 minutes of stopping reaction. The amount of cytokines in pg/ml was calculated from calibration curve created by serial dilution of interleukine standards. The experiments were repeated 3 times using supernatants of independent cultures. TNFα was not detected in the supernatants (data not shown).

Determination of cellular differentiation by flow cytometry

SZ95 cells were cutured in 6-well plates and exposed to various treatments for 24 hrs. Then, cells were stained with Nile Red (1 µg/ml Nile Red solution in PBS) for 30 minutes. Following staining, cells were harvested and subjected to flow cytometry in a NovoCyte Flow Cytometer (ACEA Biosciences, San Diego, CA, USA) using a 488 nm extinction laser. Side scatter and fluorescence characteristic for Nile Red via FL-2 channel were detected simultaneously and data were analyzed using FlowJo (FlowJo LLC, Ashland, OR, USA) software.

Data and statistical analysis

Unless it is stated otherwise, all data are presented as mean±SEM of the indicated sample size where n represents the number of independent biological repeats. Data analysis and plotting were carried out using Origin 9.0 (OriginLab Corporation, Northampton, MA, USA). Comparison of

means was done by two-tailed Student's t-test or, in case of multiple groups, by One-Way ANOVA followed by either Dunnett or Bonferroni *post hoc* tests, as appropriate. All statistical analyses were performed using IBM SPSS Statistics 23.0 (IBM, Armonk, NY, USA).

Supplementary references

Alestas T, Ganceviciene R, Fimmel S, Müller-Decker K, Zouboulis CC. Enzymes involved in the biosynthesis of leukotriene B4 and prostaglandin E2 are active in sebaceous glands. J. Mol. Med. 2006;84(1):75–87

Dobrosi N, Tóth BI, Nagy G, Dózsa A, Géczy T, Nagy L, et al. Endocannabinoids enhance lipid synthesis and apoptosis of human sebocytes via cannabinoid receptor-2-mediated signaling. FASEB J. 2008;22(10):3685–95

Makrantonaki E, Zouboulis CC. Testosterone metabolism to 5alpha-dihydrotestosterone and synthesis of sebaceous lipids is regulated by the peroxisome proliferator-activated receptor ligand linoleic acid in human sebocytes. Br. J. Dermatol. 2007;156(3):428–32

Szöllősi AG, Vasas N, Angyal Á, Kistamás K, Nánási PP, Mihály J, et al. Activation of TRPV3 Regulates Inflammatory Actions of Human Epidermal Keratinocytes. J. Invest. Dermatol. 2018;138(2):365–74

Zouboulis CC, Seltmann H, Neitzel H, Orfanos CE. Establishment and characterization of an immortalized human sebaceous gland cell line (SZ95). J. Invest. Dermatol. 1999;113(6):1011–20

Supplementary figures

Supplementary Figure S1

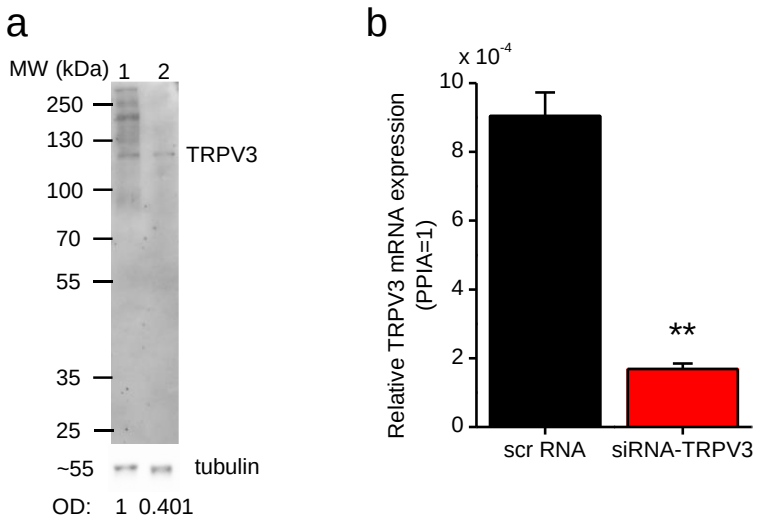

Supplementary Figure S1. RNAi-mediated silencing of TRPV3 expression in human sebocytes

SZ95 sebocytes were transfected with either scrambled RNA (scr RNA) or siRNA targeting TRPV3 (siRNA-TRPV3) as detailed in the 'Supplementary materials and methods' section. Expression of TRPV3 was checked 48 hours after transfection. a, Western blot analysis of sebocytes transfected with scrambled RNA (lane 1) or siRNA specifically targeting TRPV3 (lane 2) indicates a marked decrease of TRPV3 protein expression at 48 hours after transfection Tubulin stained on the same membrane served as a loading control to asses equal amount of total protein loaded to the PAGE. OD: relative optical density of the TRPV3 bands normalized to the corresponding tubulin bands. OD of scrambled RNA transfected sebocytes = 1. b, Quantitative analysis of TRPV3 transcripts by Q-PCR in scrambled RNA (scr RNA) and TRPV3-specific siRNA (siRNA-TRPV3) transfected sebocytes reveals a significant decrease of TRPV3 gene expression at 48 hour after transfection. N=3 independently transfected samples, **$p<0.01$ between the scr RNA and siRNA-TRPV3 transfected samples as determined by Student's t-test for independent samples. In other experiments, pharmacological treatments of scr RNA and siRNA-TRPV3-transfected cells were started 48 hours after transfection.

Supplementary Figure S2

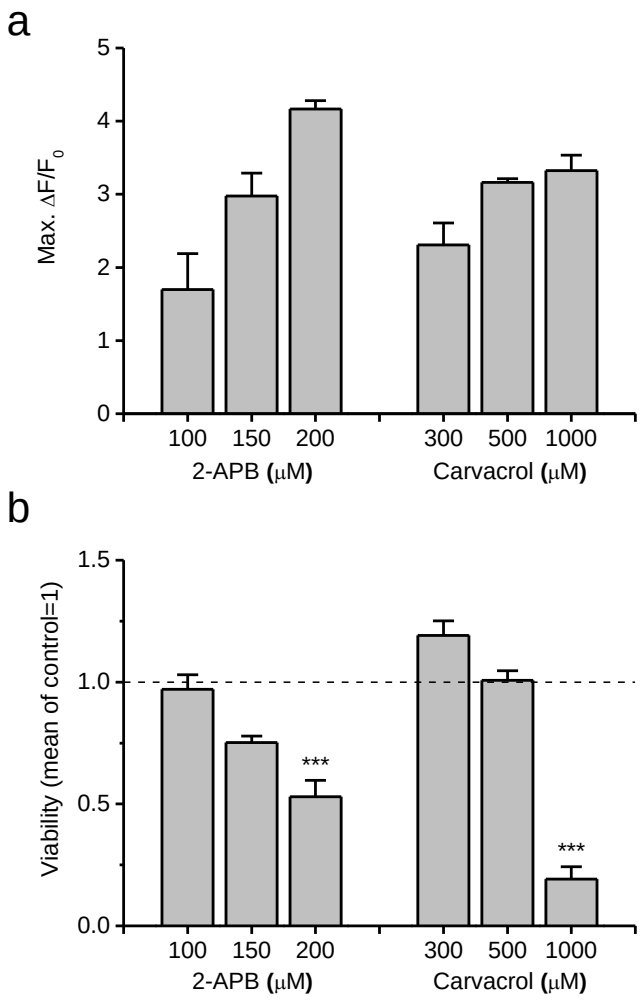

Supplementary Figure S2. Concentration dependent effect of TRPV3 agonists on cytoplasmic Ca^{2+} concentration and viability of SZ95 sebocytes

a. Statistics on the amplitude of cytoplasmic Ca^{2+} signals evoked by acute application of TRPV3 agonists in the indicated concentrations. N=3 in each group. b. Effect of the TRPV3 agonists on the viability of SZ95 cells as measured by MTT assay. N=7-8 in each group, ***$p<0.001$ compared to the vehicle treated control group as determined by One-way ANOVA and Dunnett *post hoc* test. TRPV3 agonists were applied in the same concentrations as on panel a for 24 hours prior the assay. Although high concentrations significantly reduced the MTT signal indicating declined living cell number, lower concentrations of the agonists did not decreased cellular viability after 24 hours. In other experiments, these effective but non-toxic concentrations (150 μM 2-APB and 500 μM carvacrol) were tested on lipid synthesis and cellular differentiation (24 hr-treatments) and inflammatory cytokine expression and release (6 hr-treatments).

Supplementary Figure S3

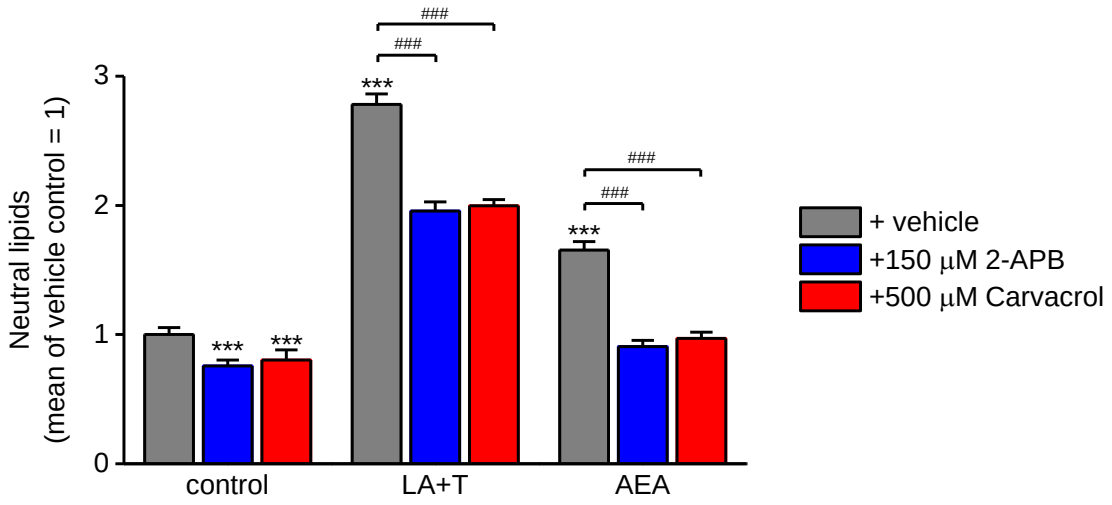

Supplementary Figure S3. Effect of TRPV3 agonists on lipid synthesis of human sebocytes

2-APB and Carvacrol were tested on the basal and induced lipogenesis of SZ95 cells. Lipogenesis was induced either by the combination of 100 µM linoleic acid and 1 µM testosterone (LA+T) (Makrantonaki and Zouboulis 2007) or by the endocannabinoid anandamide (arachidonoylethanolamine, AEA, 30 µM) (Dobrosi et al. 2008). The presence of TRPV3 agonists significantly decreased both basal and induced lipid synthesis. N≥4 in each group, ***$p<0.001$ compared to the control and $^{###}p<0.001$ between the indicated groups as determined by One-way ANOVA and Bonferroni *post hoc* test.

Supplementary Figure S4

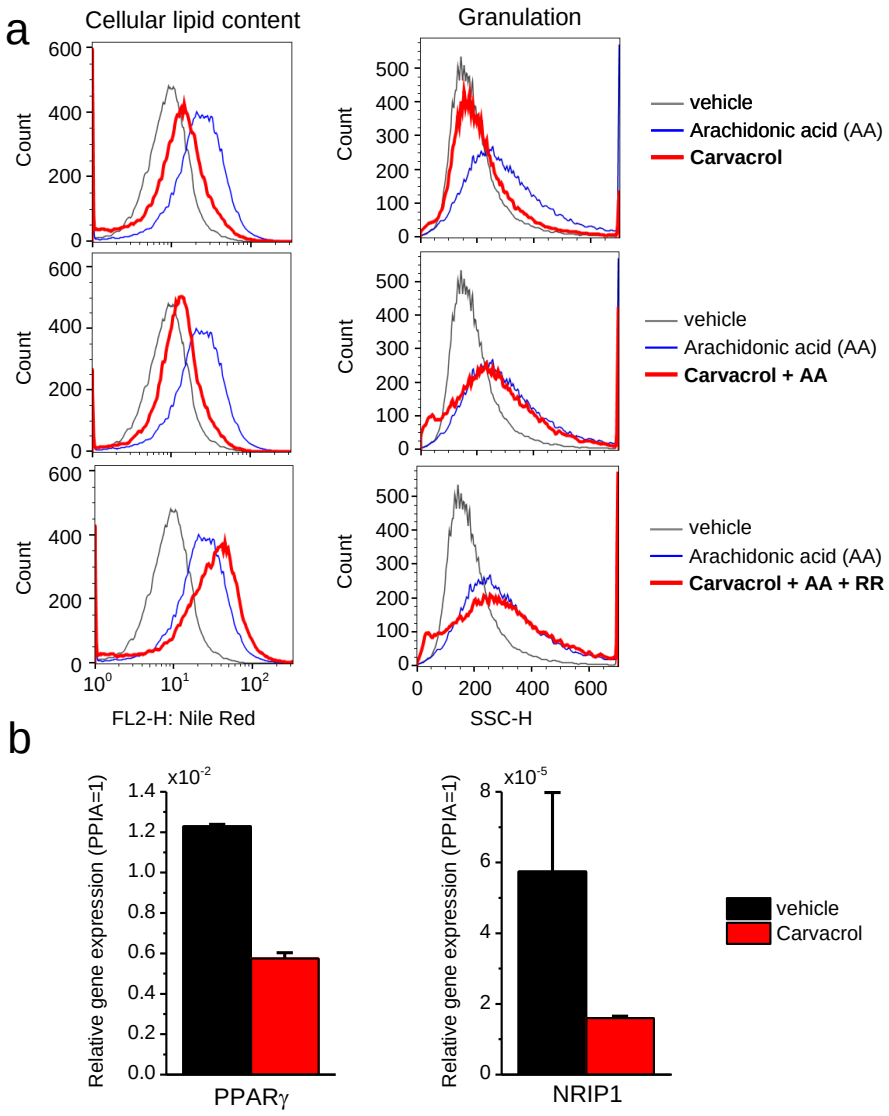

Supplementary Figure S4. Effect of TRPV3 agonist carvacrol on cellular differentiation of human sebocytes

a. SZ95 sebocytes were treated with vehicle, arachidonic acid (AA, 100 µM), carvacrol (500 µM), ruthenium red (RR, 10 µM) and combinations of the compounds as indicated in the figure for 48 hrs. Cells were stained with Nile red solution then harvested and subjected for flow cytometry as described in the Supplementary materials and methods. Fluorescence of Nile red staining and side scatter (SSC) were detected in parallel to assess cellular lipid content and granularity, respectively. AA induced a marked differentiation of the cells indicated by increased lipid accumulation and granulation of SZ95 cells. Carvacrol increased cellular lipid content only moderately, however it inhibited the AA induced cellular lipid accumulation. These effects of carvacrol were abolished by the TRPV3 blocker RR suggesting that activation of TRPV3 inhibits AA induced lipid

accumulation. In contrast, neither basal nor AA-induced granulation of sebocytes were influenced by carvacrol, suggesting that TRPV3 activation primarily affects lipid synthesis, and it has no effect on other processes of differentiation. b. Relative expression of peroxisome proliferator-activated receptor γ (PPARγ) and nuclear receptor interacting protein 1 (NRIP1) positively regulating sebaceous lipid synthesis during sebocytes' differentiation was determined by QPCR after treating cells with 500 μM carvacrol or vehicle for 24 hrs. Carvacrol markedly downregulated the expression of genes regulating lipid synthesis. N=3 independent determinations.